Large Eddy Simulation of self excited azimuthal modes in annular combustors.

Staffelbach G. ⋆, Gicquel L. Y. M. ⋆, Boudier G.⋆ and Poinsot T. J.†

⋆ *CERFACS, 42 Avenue G. Coriolis, 31057 Toulouse cedex, France*
† *Institut de Mécanique des Fluides de Toulouse, Avenue C. Soula, 31400 Toulouse, France*

Abstract

While most academic set ups used to study combustion instabilities are limited to single burners and are submitted mainly to longitudinal acoustic modes, real gas turbines exhibit mostly azimuthal modes due to the annular shape of their chambers. This study presents a massively parallel Large Eddy Simulation (LES) of a full helicopter combustion chamber in which a self-excited azimuthal mode develops naturally. The whole chamber is computed from the diffuser outlet to the High Pressure Stator nozzle. LES captures this self-excited instability and results (unsteady pressure RMS and phase fields) show that it is characterized by two superimposed rotating modes with different amplitudes. These turning modes modulate the flow rate through the fifteen burners and the flames oscillate back and forth in front of each burner, leading to local heat release fluctuations. LES demonstrates that the first effect of the turning modes is to induce longitudinal pulsations of the flow rates through individual burners. The transfer functions of all burners are the same and no mechanism of flame interactions between burners within the chamber is identified.

Keywords: azimuthal modes, swirled combustion, annular gas turbines, flame response.

1. Introduction

In the highly competitive field of power generation, gas turbines have gained an increasing role over the years. New emission regulations and growing energy demand increase the weight on the research and development of gas turbine. Substantial advances have been made and ever more complex designs have been developed to meet the increasingly stringent regulations. Unfortunately, new designs sometimes are subject to combustion instabilities [1–4]. In the case of annular combustion chambers containing multiple burners, these instabilities often take the form of azimuthal modes. These instabilities need to be predicted to evaluate their effects on the turbine operation. They also raise fundamental issues in terms of mechanisms and modeling:

- Modes appearing in annular combustion cham-

bers are often controlled by the first (and sometimes second) azimuthal acoustic mode [5–7]. These modes can appear as standing wave modes or rotating modes. Both cases are observed in gas turbines [4]. Paschereit et al [7, 8] propose a non-linear theoretical approach showing that standing wave modes can be found at low oscillation amplitudes but that only one rotating mode is found for large amplitude limit cycles.

- The models used to predict stability in annular chambers are usually based on a one-dimensional network view of the chamber in which each burner is only influenced by the flow rate fluctuation it is submitted to by the azimuthal acoustic mode. All burners are supposed to have the same transfer function (ie the same relation between inlet burner velocity and reaction rate fluctuations). This may not be the case in practice: in liquid-fueled rocket engines ormore generally in burners containing multiple jets [9], the interaction between neighbouring flames can lead to instability. This may happen in gas turbines too and require other modeling approaches than the existing ones.

Using experiments to study these issues is difficult because azimuthal modes cover the complete span of the combustion chamber and such test rigs are expensive and rare. A new approach is now possible using massively parallel computations and Large Eddy Simulation (LES). A compressible LES solver has the capacity to predict instabilities in a reacting flow configuration [3, 10]. By running such a code on a massively parallel machine (typically around 1000 processors), it is now possible to compute a full combustion chamber and study the mechanisms leading to the growth of azimuthal instabilities. In this paper a full combustion chamber LES of an helicopter turbine is presented. The LES tool and the models are first described before presenting the configuration which is a helicopter chamber demonstrator. The LES results are described next before measuring the transfer functions of each individual burner in the chamber and verifying if burners respond similarly to perturbations or if interactions between burners lead to a more complex instability mechanism.

2. LES and Numerical models

Recent studies using LES have shown the potential of this approach for reacting flows (see reviews in [3] or [11]). LES is able to predict mixing [12–16], stable flame behaviour [17–20] and flame acoustic interaction [15, 21]. It is also used for flame transfer function evaluation [22, 23]. Here a fully compressible unstructured explicit code is used to solve the multi-species Navier-Stokes equations with realistic thermochemistry on unstructured grids[24]. Multiple validations of the LES tool have been published [12, 21, 25] and are not included in the present paper. The classical Smagorinsky approach [26] is used to model the sub-grid stresses. Chemistry is accounted for with a reduced one-step scheme for JP10 / air flames fitted to match the full scheme's behavior for equivalence ratios ranging from 0.4 to 1.5. Five species are explicitly solved for: $JP10$, O_2, CO_2, H_2O and N_2. Turbulence/flame interaction is modeled with the Dynamic Thickened Flame model (DTF) [15, 24, 27, 28]. The boundary conditions are based on a multi-species extension of the NSCBC approach [29, 30]. All wall boundaries use a logarithmic law-of-the-wall formulation [15]. In this compressible solver, acoustic waves are explicitly resolved: the time step is limited by the acoustic CFL condition and a high-order spatial and temporal scheme is used to propagate acoustic waves with precision [30] so that flame/ acoustics interaction is captured correctly.

3. Target configuration

This study focuses on a full helicopter combustion chamber equipped with fifteen burners (Fig 1). Each burner contains two co-annular counter-rotating swirlers (Fig 2). The fuel injectors are placed in the axis of the swirlers. To avoid uncertainties on boundary conditions the chamber's casing is also computed so that the computational domain starts after the inlet diffuser and ends at the throat of the high pressure stator which is choked. The air and fuel inlets use non-reflective boundary conditions [29]. The air flowing at 578K in the casing feeds the combustion chamber through the swirlers, films and dilution holes. To simplify the LES, fuel is supposed to be vaporized at the lips of the injector and no model is used to describe liquid kerosene injection, dispersion and vaporization.
Each burner is numbered starting with sector 1 placed at z=0 and y $>$ 0. The sector number increases clockwise. Specific data will be shown for the burners on two locations referred to as probe A_i and probe B_i (Fig. 1) with i being the burner indice and going from 1 to 15. Type A_i probes are located in the chamber casing and B_i probes are located in each burner's axis at the end of the burner.

4. LES of a self-excited azimuthal mode

The full chamber (fifteen sectors and burners) LES is initialised using a single sector LES with periodic boundary conditions which is copied over the other fourteen sectors. The final mesh contains 9 009 065 nodes and 42 287 640 elements. The time step for this configuration is 0.067 microseconds and the typical CPU cost is 3.96 hours on 700 processors of a CRAY XT 3 machine for one period of the azimuthal mode.
A snapshot of the temperature field on a cylindrical plane passing through the B_i probes is displayed on Fig. 3. The isocontours correspond to the velocity magnitude. A direct observation of this field versus time (not shown here) reveals that, when the LES

is converged, the flames oscillate azimuthally, moving from left to right at a frequency close to $740Hz$. This azimuthal motion is accompanied by an axial displacement of all flames displayed in Fig. 4. This figure shows an instantaneous temperature and pressure field which reveals that the flames distances to the burners exit planes change: certain flames are very close to the burners (left side Fig. 4) while others are lifted (right side Fig. 4). This pattern oscillates at the frequency of the azimuthal mode.

Figure 5 shows the time variations of the transverse velocity component for probe A_1. When the LES begins on the full combustor geometry, a strong oscillation of the transverse velocity component appears at 740 Hz. This frequency matches the value of the first azimuthal mode which can be obtained with a Helmholtz solver using the mean temperature distribution in the combustor [31, 32]. It can also be estimated simply by : $f = \frac{c}{2\pi r}$ where c is the sound speed in the chamber and r the chamber radius. Here $c \approx 900m.s^{-1}$, $r \approx 0,2m$ so that $f \approx 720Hz$ which is close to the observed LES value of $740Hz$.

The reduced temperature ($\frac{T}{Tmean}$) signals on probes B_1, B_6 and B_9 confirm that the flames periodically flash back into the burners (Fig. 6). Figure 7 shows reduced mass flow and heat release rates over time for burners 2, 7 and 11 and reveals strong sinusoidal fluctuations of the mass flow rates and strong non linear heat release fluctuations. The flow rate fluctuations obviously control the flame response and the heat release perturbation. This is confirmed by Fig. 8 which shows (for sector 1) the flame position over time compared to the mass flow rate through the burner and Fig. 9 which shows (for sector 1 again) the heat release and the pressure fluctuations. All values here are normalized by their average and maximum values ($\bar{f} = \frac{f - f_{average}}{f_{max} - f_{average}}$). When the mass flow rate is minimum, the pressure is maximum: the flame has propagated upstream and its distance to the burner inlet is minimum. Sometimes, this can lead to flashback but not for all burners and not for all cycles: during these flashback events (Fig. 4), the flame enters the injector (Fig. 2) and stops at the tip of the swirlers. When the flow rate increases, the flame is pushed downstream, leading to a maximum heat release 180 degrees after the instant of maximum flow rate (Fig 7). The phase difference between the pressure and the heat release is of the order of 90 degrees so that the Rayleigh criterion is locally satisfied for the fifteen sectors.

Figure 10 shows the pressure amplitude for all B_i probes and Fig. 11 shows the phase between the pressure signal at probes A_i and probe A_1 which is used as reference. The almost linear phase suggests the presence of a rotating azimuthal mode but the pressure variation suggests that a second (counter-rotating) acoustic mode is also present. A simple model can be used to recover the amplitude and phase of the pressure signals found in the LES for the different burners by considering two counter-rotating acoustic modes P_+ and P_- such that:

$$P_+ = A_+ \cdot e^{i \cdot k \cdot \theta - i\omega t} \quad \text{and} \quad \mathrm{P_-} = \mathrm{A_-} \cdot \mathrm{e}^{-\mathrm{i \cdot k \cdot \theta - i\omega t}} \qquad (1)$$

When $A_- = 0.33A_+$, the amplitude and phase of the resulting acoustic pressure $P_+ + P_-$ compare very well to the LES data (Fig. 10 and 11). This simple model suggests that the LES captures two rotating modes: the first one (clockwise) dominates while the second one (counterclockwise) has an amplitude of one third of the first one. Why this is so is unclear at the moment. Note that the full geometry LES is not axisymmetric: the fifteen swirlers do have a common rotation sense (which is clockwise when looking from the swirlers to the chamber) so that there are reasons to expect modes of different amplitudes. There is actually a mean azimuthal clockwise flow in the chamber as evidenced by the fact that the transverse velocity component (Fig. 5) stabilizes around a non-zero mean value (typically 1.5 m/s which is a small but non negligible rotation movement). More modeling and LES analysis is required now to explain why the clockwise mode dominates. What is clear however from the present results is that two rotating modes co exist and that these modes induce an axial forcing of the mass flow rates in the fifteen burners and a subsequent oscillation of the heat release in each sector which satisfies the Rayleigh criterion.

5. Individual burner transfer function

Since each burner is axially forced by the azimuthal acoustic mode, it is possible to evaluate its response to the flow rate oscillations by computing the transfer function between inlet velocity fluctuations $u = \hat{u}e^{-i\omega t}$ and global sector unsteady heat release $\Omega = \hat{\Omega}e^{-i\omega t}$. Ω is the unsteady heat release averaged in each sector and u the bulk velocity through each burner. Figure 12 shows the modulus n and the phase τ of $\hat{\Omega}/\hat{u}$ for each of the fifteen burners.

Amplitudes and delays are fairly constant with $n = 4.6MW.m^{-2}.s^{-1}$ and $\tau = 0.58ms$ suggesting a unique response for all burners. This has important implications:

1. First, this shows that during a limit cycle induced by an azimuthal mode, each burner reacts only to axial flow rate perturbations: even though the mode structure is azimuthal, the burners response is only due to the modulation of the flow rate passing through the injector. No other mechanism (like the interaction between flames issuing from neighbouring burners [9]) seems to be present in this setup.
2. Second, this confirms that models based on simple quasi-dimensional network views of the annular chamber are adequate to study the stability of annular combustion chambers [33, 34].
3. Third, the main difficulty in building network acoustic models is to determine the response of individual burners [35–39]. The present results show that this response is the response of a

burner submitted to an axial flow rate perturbation. Therefore, it can be determined by an LES or an experiment performed on a single sector. This simplification is extremely useful because it provides a simple method (with only single burner experiments or LES) to predict the stability of a full annular chamber.

6. Conclusion

A full combustion chamber LES of an helicopter chamber was performed using massively parallel computing. Including the chamber's casing, the swirlers and the choked high pressure stator reduces uncertainties on boundary conditions. The LES reveals that a self-excited mode at 740Hz grows and reaches a limit cycle where two counter-rotating modes with different amplitudes modulate the flow rate through the fifteen burners. This leads to strong modulations of the flame position and sometimes to flashback. The LES also shows that the transfer functions of all burner are identical. This confirms that the effects of the azimuthal mode is mainly translated into an axial fluctuation of the flow rates through the injectors and that simple network models can be used in such geometries. It also shows that, since the burners are only affected by flow rate oscillations, their response can be obtained by single burner LES or experiments, thereby allowing a prediction of the stability of full annular chambers during design without having to actually build them or compute them.

Acknowledgment

The authors wish to acknowledge the help of Turbomeca (Dr C. Berat and Dr V. Moureau). Special thanks to the Barcelona Computing Center and to Cray Inc. for providing the computer power necessary for this simulation.

References

[1] S. Candel, in: *24th Symp. (Int.) on Combustion*, The Combustion Institute, Pittsburgh, 1992, pp. 1277–1296.

[2] D. Crighton, A. Dowling, J. Ffowcs Williams, M. Heckl, F. Leppington, *Modern methods in analytical acoustics*, Lecture Notes, Springer Verlag, New-York, 1992.

[3] T. Poinsot, D. Veynante, *Theoretical and numerical combustion*, R.T. Edwards, 2nd edition., 2005.

[4] T. Lieuwen, V. Yang, *Combustion Instabilities in Gas Turbine Engines. Operational Experience, Fundamental Mechanisms and Modeling*, Vol. 210, AIAA, 2005.

[5] S. Stow, A. Dowling, in: *ASME Paper*, New Orleans, Louisiana, 2001.

[6] W. Krebs, P. Flohr, B. Prade, S. Hoffmann, *Combust. Sci. Tech.* 174 (2002) 99–128.

[7] B. Schuermans, C. Paschereit, P. Monkiewitz, Vol. AIAA paper 2006-0549, 2006.

[8] B. Schuermans, V. Bellucci, C. Paschereit, in: *International Gas Turbine and Aeroengine Congress & Exposition, ASME paper*, Vol. 2003-GT-38688, 2003.

[9] T. Poinsot, A. Trouvé, D. Veynante, S. Candel, E. Esposito, *J. Fluid Mech.* 177 (1987) 265–292.

[10] L. Selle, G. Lartigue, T. Poinsot, R. Koch, K.-U. Schildmacher, W. Krebs, B. Prade, P. Kaufmann, D. Veynante, *Combust. Flame* 137 (4) (2004) 489–505.

[11] H. Pitsch, *Ann. Rev. Fluid Mech.* 38 (2006) 453–482.

[12] C. Prière, L. Gicquel, A. Kaufmann, W. Krebs, T. Poinsot, *J. Turb.* 5 (2004) 1–30.

[13] C. Pierce, P. Moin, *Phys. Fluids* 10 (12) (1998) 3041–3044.

[14] H. Pitsch, H. Steiner, *Phys. Fluids* 12 (2000) 2541–2554.

[15] P. Schmitt, T. Poinsot, B. Schuermans, K. Geigle, *J. Fluid Mech.* 570 (2007) 17–46.

[16] B. Vreman, B. Geurts, H. Kuerten, *International Journal for Numerical Methods in Fluids* 22 (1996) 297–311.

[17] W. Kim, S. Menon, *Int. J. Num. Meth. Fluids* 31 (1999) 983–1017.

[18] W. Kim, S. Menon, H. Mongia, *Combust. sci. technol.* 143 (1-6) (1999) 25–62.

[19] H. Forkel, J. Janicka, *Flow Turb. and Combustion* 65 (2) (2000) 163–175.

[20] N. Branley, W. P. Jones, *Combust. Flame* 127 (2001) 1914–1934.

[21] L. Selle, F. Nicoud, T. Poinsot, *AIAA Journal* 42 (5) (2004) 958–964.

[22] A. Kaufmann, F. Nicoud, T. Poinsot, *Combust. Flame* 131 (2002) 371–385.

[23] L. Selle, L. Benoit, T. Poinsot, F. Nicoud, W. Krebs, *Combust. Flame* 145 (1-2) (2006) 194–205.

[24] O. Colin, M. Rudgyard, *J. Comput. Phys.* 162 (2) (2000) 338–371.

[25] S. Roux, G. Lartigue, T. Poinsot, U. Meier, C. Bérat, *Combust. Flame* 141 (2005) 40–54.

[26] J. Smagorinsky, *Monthly Weather Rev.* 91 (1963) 99–164.

[27] O. Colin, F. Ducros, D. Veynante, T. Poinsot, *Phys. Fluids* 12 (7) (2000) 1843–1863.

[28] J.-P. Légier, T. Poinsot, D. Veynante, in: *Summer Program 2000*, Center for Turbulence Research, Stanford, USA, 2000, pp. 157–168.

[29] T. Poinsot, S. Lele, *J. Comput. Phys.* 101 (1) (1992) 104–129.

[30] V. Moureau, G. Lartigue, Y. Sommerer, C. Angelberger, O. Colin, T. Poinsot, *J. Comput. Phys.* 202 (2) (2005) 710–736.

[31] L. Benoit, F. Nicoud, *Int. J. Numer. Meth. Fluids* 47 (8-9) (2005) 849–855.

[32] F. Nicoud, L. Benoit, C. Sensiau, *AIAA Journal* 45 (2007) 426–441.

[33] A. Dowling, *J. Sound Vib.* 180 (4) (1995) 557–581.

[34] S. Evesque, W. Polifke, in: *International Gas Turbine and Aeroengine Congress & Exposition, ASME paper*, Vol. GT-2002-30064, 2002.

[35] A. Birbaud, D. Durox, S. Ducruix, S. Candel, *Proc. of the Combustion Institute* 31 (2007) 1257–1265.

[36] S. Hemchandra, T. Lieuwen, *Proc. of the Combustion Institute* 31 (2007) 1427–1434.

[37] C. Paschereit, W. Polifke, B. Schuermans, O. Mattson, *J. Eng. for Gas Turb. and Power* 124 (2002) 239–247.

[38] W. Polifke, A. Poncet, C. Paschereit, K. Doebbeling, *J. Sound Vib.* 245 (3) (2001) 483–510.

[39] T. Lieuwen, Y. Neumeier, in: *Proceedings of the Combustion Institute*, Vol. 29, 2002, pp. 99–105.

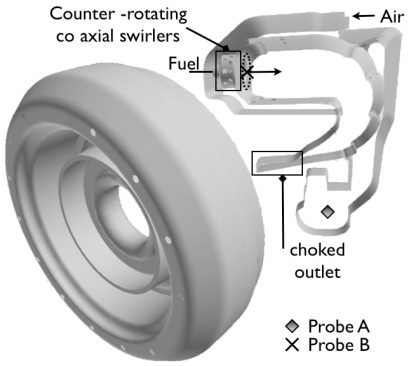

Fig. 1: Gas turbine geometry, Boundary conditions and post-processing tools positions.

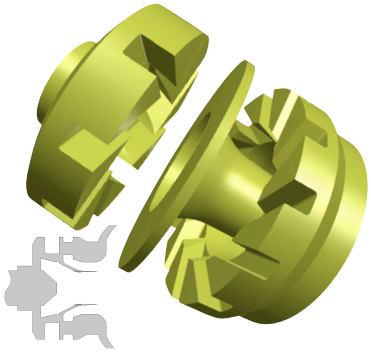

Fig. 2: Detailed view of the swirlers.

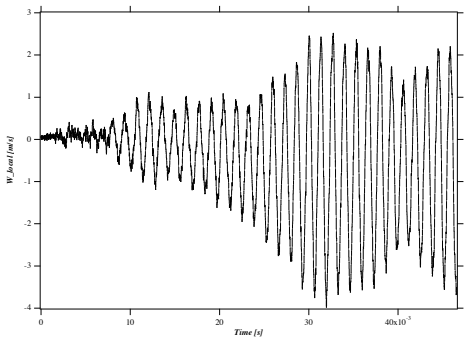

Fig. 5: Transverse velocity component at probe type A of sector 1.

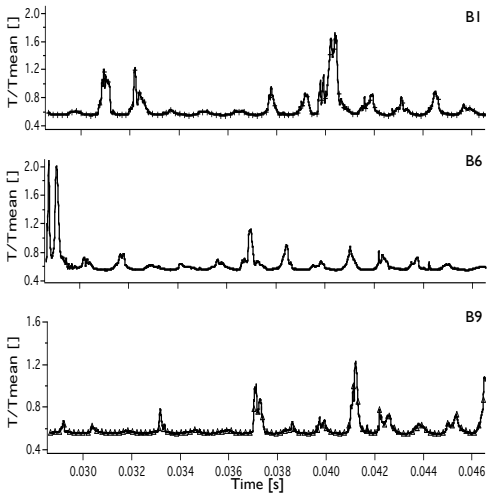

Fig. 6: $\frac{T}{Tmean}$ over time for probes B_1, B_6 and B_9.

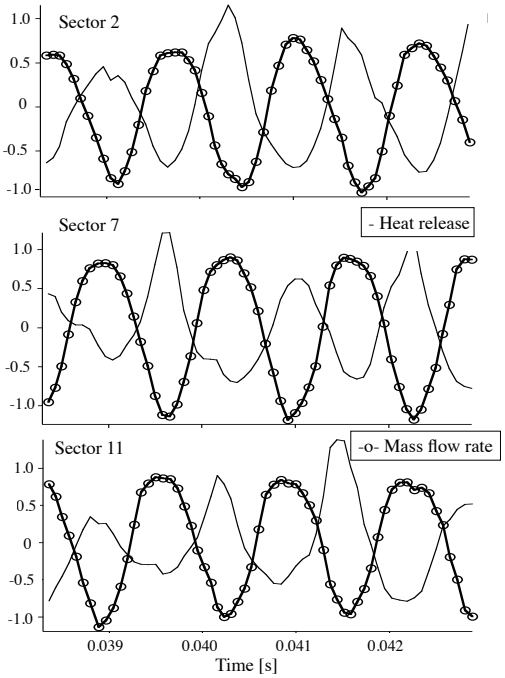

Fig. 7: Mass flow rate and Heat release fluctuations for sectors 2, 7 and 11: - Heat release, • Mass flow rate.

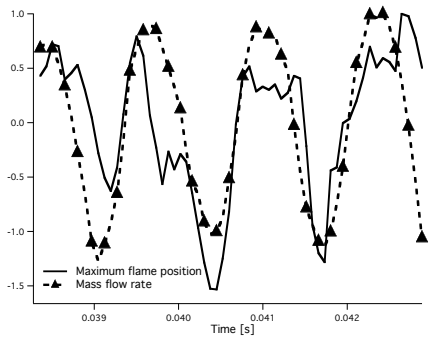

Fig. 8: Sector 1 : - Maximum flame position (First abscissa along the burner axis where Tmean is reached), ♦ Average heat release in sector 1.

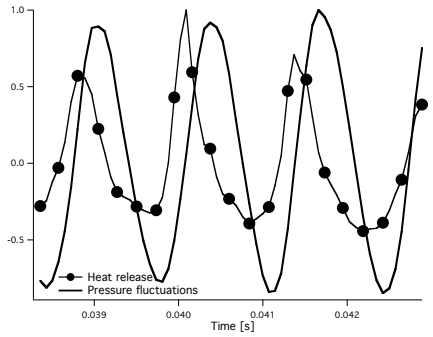

Fig. 9: Sector 1 : • Heat release, - Pressure fluctuation average in the sector.

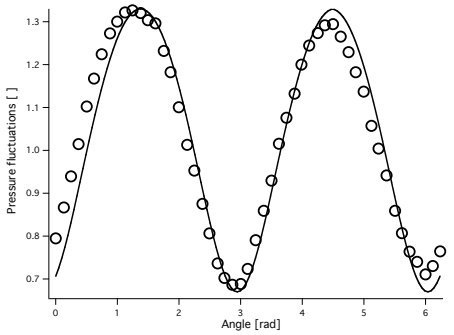

Fig. 10: $\frac{Prms}{Pmean}$ for all B_i probes : - model, ○ LES.

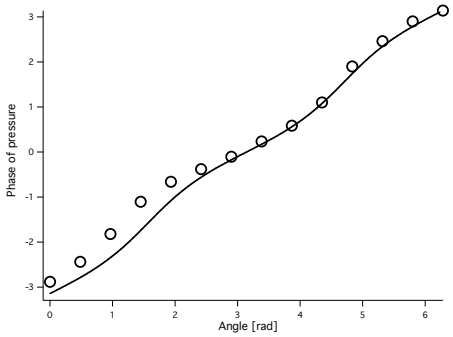

Fig. 11: Pressure signal phase (sector 1 is used as reference): - model, ○ LES.

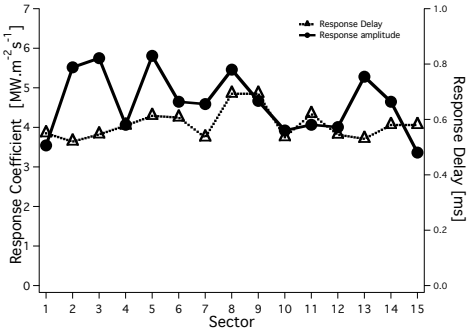

Fig. 12: Sector by sector flame response to the self-exited mode: ○ Response amplitude • Response delay (ms).

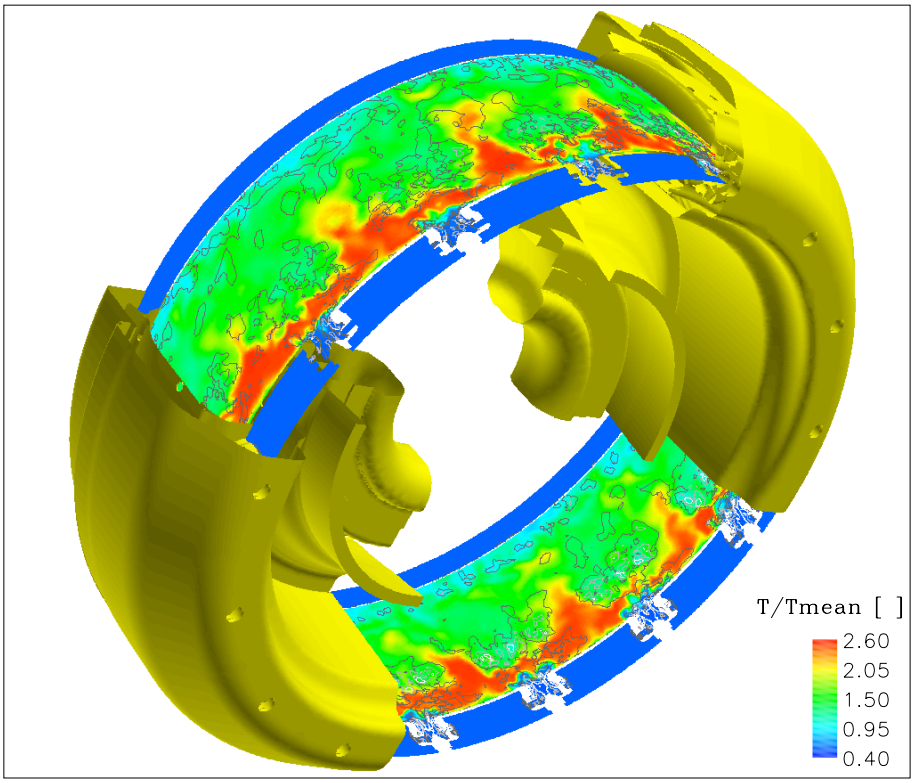

Fig. 3: 3D view of the computational domain, Temperature field on a cylindrical plane passing through the B_i probes. Velocity magnitude isocontours.

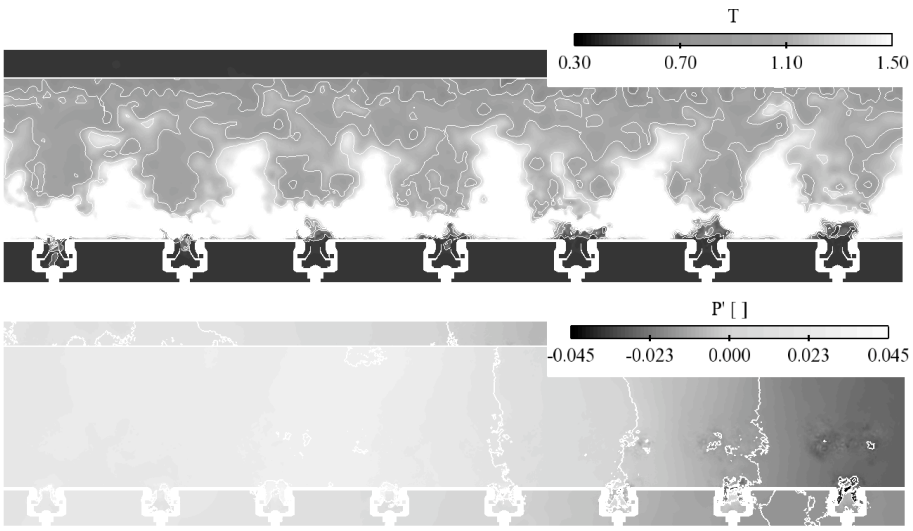

Fig. 4: Detailed view of half of the burners. top : Temperature field with temperature isocontour. Bottom: Pressure fluctuations with P'=0 isoline.